# Potent Protection against Aflatoxin-Induced Tumorigenesis through Induction of Nrf2-Regulated Pathways by the Triterpenoid 1-[2-Cyano-3-,12-Dioxooleana-1,9(11)-Dien-28-Oyl]Imidazole

Melinda S. Yates,[1] Mi-Kyoung Kwak,[1] Patricia A. Egner,[1] John D. Groopman,[1] Sridevi Bodreddigari,[2] Thomas R. Sutter,[2] Karen J. Baumgartner,[3] B.D. Roebuck,[3] Karen T. Liby,[3] Mark M. Yore,[3] Tadashi Honda,[4] Gordon W. Gribble,[4] Michael B. Sporn,[3] and Thomas W. Kensler[1]

[1]Johns Hopkins University, Baltimore, Maryland; [2]University of Memphis, Memphis, Tennessee; and [3]Dartmouth Medical School and [4]Dartmouth College, Hanover, New Hampshire

## Abstract

**Synthetic triterpenoid analogues of oleanolic acid are potent inducers of the phase 2 response as well as inhibitors of inflammation. We show that the triterpenoid, 1-[2-cyano-3-,12-dioxooleana-1,9(11)-dien-28-oyl]imidazole (CDDO-Im), is a highly potent chemopreventive agent that inhibits aflatoxin-induced tumorigenesis in rat liver. The chemopreventive potency of CDDO-Im was evaluated by measuring inhibition of formation of putative preneoplastic lesions (glutathione _S_-transferase P positive foci) in the liver of rats exposed to aflatoxin $B_1$. CDDO-Im produces an 85% reduction in the hepatic focal burden of preneoplastic lesions at 1 $\mu$mol/ kg body weight and a >99% reduction at 100 $\mu$mol/kg body weight. CDDO-Im treatment reduces levels of aflatoxin-DNA adducts by ~40% to 90% over the range of 1 to 100 $\mu$mol/kg body weight. Additionally, changes in mRNA levels of genes involved in aflatoxin metabolism were measured in rat liver following a single dose of CDDO-Im. _GSTA2_, _GSTA5_, _AFAR_, and _EPHX1_ transcripts are elevated 6 hours following a 1 $\mu$mol/kg body weight dose of CDDO-Im. Microarray analysis using wild-type and _Nrf2_ knockout mice confirms that many phase 2 and antioxidant genes are induced in an Nrf2-dependent manner in mouse liver following treatment with CDDO-Im. Thus, low-micromole doses of CDDO-Im induce cytoprotective genes, inhibit DNA adduct formation, and dramatically block hepatic tumorigenesis. As a point of reference, oltipraz, an established modulator of aflatoxin metabolism in humans, is 100-fold weaker than CDDO-Im in this rat antitumorigenesis model. The unparalleled potency of CDDO-Im _in vivo_ highlights the chemopreventive promise of targeting Nrf2 pathways with triterpenoids.** (Cancer Res 2006; 66(4): 2488-94)

## Introduction

Induction of phase 2 enzymes is an effective mechanism of protection against carcinogenesis, mutagenesis, and other forms of toxicity mediated by carcinogens. Phase 2 enzymes, such as glutathione _S_-transferases (GST) and UDP-glucuronosyl transferases, are involved in the metabolism of carcinogens and function to facilitate their elimination. The protective effects of phase 2 enzyme induction have been shown in a wide variety of models. For example, oltipraz and related dithiolethiones are potent phase 2 inducers that protect against acute toxicity caused by acetaminophen, allyl alcohol, and aflatoxin in mice, hamsters, and rats, respectively. Dithiolethiones are also chemoprotective in animal models of chemically induced carcinogenesis targeting liver, lung, colon, small intestine, forestomach, bladder, mammary glands, and skin (1). Dithiolethiones are especially effective at inhibiting aflatoxin-induced hepatocarcinogenesis in rats (2). Furthermore, the feasibility and potential importance of phase 2 enzyme induction has been confirmed in humans. Several studies have shown that oltipraz modulates phase 2 enzymes in humans (3). GST activity is doubled in peripheral lymphocytes after dosing with 125 mg oltipraz (4). Increased GST activity in peripheral mononuclear cells and colon mucosa biopsies following treatment with oltipraz has also been reported (5). Clinical trials of oltipraz have been conducted in residents of Qidong, People's Republic of China, who are at increased risk for development of hepatocellular carcinoma, in part due to consumption of aflatoxin-contaminated foods, such as corn and peanuts. Oltipraz increased phase 2 conjugation of the ultimate carcinogenic species, aflatoxin-8,9-oxide, yielding higher rates of excretion of aflatoxin-mercapturic acid in urine (6). Increased formation of the aflatoxin-mercapturic acid results from GST conjugation of the epoxide and is inversely associated with levels of aflatoxin DNA adducts formed in liver and excreted into urine.

The mechanisms that result in protection by dithiolethiones and other classes of phase 2 inducers are under investigation. The Keap1-Nrf2 signaling pathway seems to play a central role in the constitutive and inducible expression of many phase 2 genes, including GSTs (7). Inducers may interact with critical cysteines in Keap1 through oxidoreduction or alkylation, allowing the transcription factor Nrf2 to escape proteosomal degradation and to accumulate in the nucleus. In turn, Nrf2 binds as heterodimers with small Maf proteins to the antioxidant response elements (ARE) found in the promoter regions of many phase 2 genes. Comparative genomic studies in wild-type and _Nrf2_-disrupted mice have revealed that Nrf2 regulates the inducible expression of multiple categories of genes, including antioxidative/anti-inflammatory genes, molecular chaperones/stress response genes, proteasome subunit genes, as well as carcinogen-metabolizing enzymes (8). The multiple components of such a broad-based adaptive response allow for protection against electrophile and oxidant stresses, both of which are components of carcinogenesis. _Nrf2_-deficient mice are greatly predisposed to chemically induced DNA damage and exhibit higher susceptibility toward cancer

development in several models of chemical carcinogenesis (9). Moreover, *Nrf2*-disrupted mice are refractory to the protective effects of inducers, such as oltipraz, highlighting the importance of the Keap1-Nrf2-ARE signaling pathway as a molecular target for prevention.

Oleanolic acid is a naturally occurring triterpenoid. Several of its synthetic analogues have marked anti-inflammatory and antitumorigenic activities, mediated in part through Nrf2 signaling. Thus, Dinkova-Kostova et al. (10) have recently reported that several triterpenoid analogues are extremely potent inducers of phase 2 enzymes *in vitro*, with induction observed at subnanomolar concentrations. Although these triterpenoid analogues induce quinone reductase (NQO1) activity and inhibit nitric oxide production in wild-type mouse embryonic fibroblast cells, they are inactive in *Nrf2* knockout cells (10). Haridas et al. (11) showed that treatment with triterpenoid electrophiles, called avicins, causes enhanced expression of stress response proteins and increased nuclear localization of Nrf2. Further studies were conducted *in vivo* in mouse skin exposed to UV light. These studies showed that triterpenoid treatment resulted in inhibition of epidermal hyperplasia, reduced p53 mutation, and enhanced apoptosis. Liby et al. (12) has reported that two of the most potent synthetic triterpenoid analogues, 2-cyano-3,12-dioxooleana-1,9(11)-dien-28-oic acid (CDDO) and its imidazolide derivative 1-[2-cyano-3-,12-dioxooleana-1,9(11)-dien-28-oyl]imidazole (CDDO-Im) activate a number of genes regulated by Nrf2. These studies also show that low concentrations of CDDO-Im reduce formation of reactive oxygen species in U937 cells, as well as *Nrf2* wild-type cells, whereas reactive oxygen species levels are unchanged in *Nrf2* knockout cells. Interestingly, *Nrf2* wild-type and knockout fibroblasts show no difference in growth inhibition following treatment with CDDO or CDDO-Im, indicating that Nrf2 does not mediate all of the actions of these triterpenoids. Triterpenoid analogues have shown an array of promising activities in other models as well. CDDO inhibits growth and induces cell cycle arrest in breast cancer cell lines (13). In addition, CDDO treatment induces apoptosis in breast cancer and leukemic cell lines (13, 14). CDDO also induces differentiation of human myeloid leukemia cells and mouse 3T3-L1 fibroblasts (15). In melanoma and leukemia mouse models, treatment with CDDO-Im inhibits tumor growth (16).

The pronounced activity of triterpenoids *in vitro* prompted us to evaluate the potency of CDDO-Im (Fig. 1) in a highly quantitative model for cancer chemoprevention *in vivo*. Using a rat model of aflatoxin-induced carcinogenesis extensively validated during the preclinical development of dithiolethiones, we are able to evaluate the chemopreventive potency of CDDO-Im by measuring inhibition of preneoplastic lesions (GST-P positive foci) in the liver of rats exposed to aflatoxin. Because of the well-characterized role of
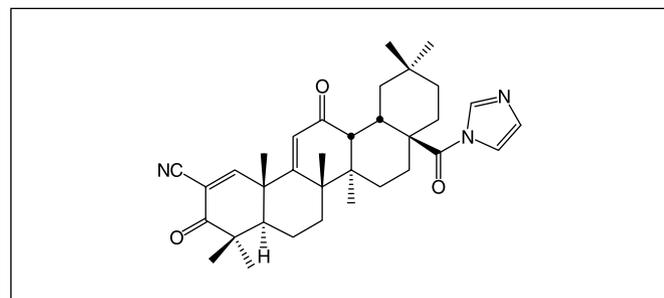


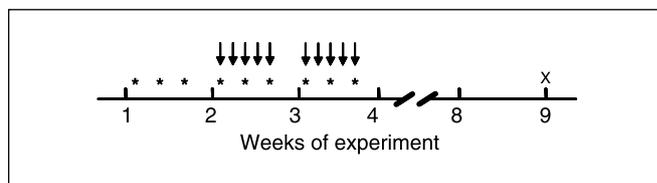**Figure 1.** Chemical structure of CDDO-Im.



**Figure 2.** Protocol for evaluating CDDO-Im as an inhibitor of aflatoxin-induced tumorigenesis. *, gavage of CDDO-Im.    gavage of AFB₁, 25 µg/rat/d. *X,* time of sacrifice.

aflatoxin metabolism in this carcinogenesis model, we are also able to probe the mechanism of protection by measuring the dose-response characteristics of inhibition of aflatoxin-DNA adduct formation as well as changes in mRNA and protein levels of associated cytoprotective genes. Companion studies in mice indicate the important role of Nrf2 genotype on the expression of cytoprotective genes. Collectively, our results indicate that CDDO-Im is an exceptionally potent chemopreventive agent *in vivo*.

## Materials and Methods

**Animals.** Male F344 rats (85-110 g) were purchased from Harlan (Indianapolis, IN). ICR wild-type and *Nrf2*-disrupted mice were generated from inbred *Nrf2*-heterozygous mice (17). Animals were fed AIN-76A purified diet without ethoxyquin. All experiments were approved by The Johns Hopkins University Animal Care and Use Committee.

**Chemicals.** CDDO-Im was synthesized as previously described (18–20). Aflatoxin B₁ (AFB₁) was obtained from Sigma-Aldrich (St. Louis, MO).

**AFB-DNA adduct inhibition.** Rats were gavaged with 1, 3, 10, 30, or 100 µmol CDDO-Im/kg body weight using a vehicle of 10% DMSO, 10% Cremophor-EL, and PBS. Forty-eight hours after treatment with CDDO-Im, rats were gavaged with 25 µg/rat of AFB₁ dissolved in DMSO. Rats were sacrificed 2 hours following treatment with AFB₁. Livers were immediately frozen in liquid nitrogen using a freeze clamp and stored at −80°C. DNA was isolated (21) and analyzed for levels of aflatoxin-DNA adducts by liquid chromatography-mass spectrometry as described previously (22). Total DNA content was measured spectrophotometrically using diphenylamine.

**Hepatic foci inhibition.** For 3 successive weeks on Monday, Wednesday, and Friday at 8:00 a.m., rats were gavaged with CDDO-Im (1, 3, 10, 30, or 100 µmol/kg body weight). Beginning on the second week, AFB₁ (25 µg/rat) was gavaged at 2:00 p.m. hours Monday through Friday for 2 weeks. Groups administered vehicle or AFB₁ without chemoprotective agent were included. Rats were sacrificed 5 weeks after the last doses of CDDO-Im and AFB₁. This protocol is presented in Fig. 2. Multiple 2-mm-thick sections were cut by hand from the left lateral lobe of the liver, fixed in 4°C acetone, and embedded in paraffin. Liver sections (5 µm thick) were stained by immunohistochemical methods for expression of GST-P positive foci and analyzed by light microscopy. As with previous analyses (23), the observed focal data of number of foci per unit tissue area and their focal transectional areas were first subjected to morphometric transformation resulting in the volume percent of liver occupied by GST-P positive foci and the less robust variables of foci per unit volume of liver and mean focal diameter. Details of this protocol have been published previously (24, 25).

**Statistical analysis.** Body weights, DNA adduct inhibition, and mRNA changes were compared among groups by ANOVA followed by the Student-Newman-Keuls test. Hepatic foci inhibition data were compared by ANOVA followed by a Bonferroni multiple comparison test. These statistics were determined only for the calculated morphometric data including volume percent. Foci were not detected in some animals treated with the highest doses of CDDO-Im. Values of $L / 2$ (limit of detection / 2) were inserted for all zero values as described (26). $L$ is defined as the lowest value observed in all groups. The lowest observed volume percentage value was 0.003.

**Gene expression analysis.** Rats were gavaged with 1, 3, 10, or 30 µmol CDDO-Im/kg body weight. Rats were sacrificed 6 or 24 hours after treatment and livers were removed. The outer halves of both the left and

right lateral lobes of the liver were immediately placed in RNA*later* (Ambion, Austin, TX). The remaining portion of the liver was freeze-clamped in liquid nitrogen and stored at −80°C for use in Western blot analyses. Total RNA was isolated from liver samples stored in RNA*later* using Versagene RNA purification kit (Gentra Systems, Minneapolis, MN) and cDNA was synthesized using iSCRIPT cDNA Synthesis kit (Bio-Rad, Hercules, CA). Gene expression measurements were accomplished using TaqMan Gene Expression Assays (Applied Biosystems, Foster City, CA) and iQ Supermix (Bio-Rad). Gene expression data from real-time quantitative PCR was analyzed using the $2^{-\Delta\Delta C_t}$ relative quantification method as published (27).

**Gel electrophoresis and immunoblotting.** Livers were homogenized in buffer containing 50 mmol/L Tris-HCl (pH 7.8), 200 mmol/L KCl, 5 mmol/L MgCl$_2$, and 1 mmol/L DTT and centrifuged at 15,000 × $g$ for 15 minutes at 4°C. Tissue homogenates were loaded on a 12% SDS-polyacrylamide gel and separated by electrophoresis.

For separation of AFB$_1$ aldehyde reductase (AFAR) and β-actin, the concentration of cross-linker *N,N′*-methylene-bis-acrylamide was 2.6% (w/w); for the separation of GST subunits, the concentration was 0.6% (w/w) as described (28). Proteins from gels were electrophoretically transferred to a 0.2 μm nitrocellulose membrane (Schleicher & Schuell, Keene, NH) with a Bio-Rad trans-blot cell. Incubation for 1 hour with the primary antibodies to AFAR (29), GSTA5 (30), or β-actin (Sigma-Aldrich, St. Louis, MO) were at dilutions of 1:500, 1:5,000, and 1:2,000, respectively. Bound antibody was detected using horseradish peroxidase–linked secondary antibody, and then quantified by enhanced chemiluminescence (Super-Signal System, Pierce, Rockford, IL; Kodak Biomax, Eastman Kodak, Rochester, NY). The signal intensities on the films were determined using Scion Image Software (Scion, Frederick, MD) and used to calculate the relative fold expression.

**Mouse microarray sample preparation.** Male wild-type and *Nrf2*-disrupted ICR mice (11-12 weeks old) were gavaged with 150 μmol CDDO-Im/kg body weight. Mice were sacrificed 24 hours after treatment. Livers were removed and snap frozen. Total RNA was purified using the Totally RNA kit (Ambion). Isolated RNA was further purified using RNeasy Mini kit (Qiagen, Valencia, CA). cDNA was synthesized using Superscript Choice kit (Invitrogen, Carlsbad, CA) with a T7-(dT)$_{24}$ primer. Biotin-labeled cRNA was prepared by *in vitro* transcription (Enzo Biochemical, New York, NY) and fragmented by incubation at 94°C for 45 minutes in 40 mmol/L Tris acetate buffer (pH 8.1), with 100 mmol/L potassium and 30 mmol/L magnesium acetate. Fragmented cRNA was hybridized at 45°C for 16 hours to a Mouse Genome 430 2.0 GeneChip (Affymetrix, Santa Clara, CA), which contains over 39,000 transcripts. Gene chips were washed and stained using a fluid station and scanned using an Affymetrix Genechip system confocal scanner.

**Microarray data analysis.** Affymetrix GeneChip Operating Software (GCOS v1.1.1) was used for analysis. Pairwise comparisons of individual mice ($n$ = 3) were done, generating nine comparisons. A coefficient of variation (CV = SD / mean) value of 1.0 was used as a preliminary filter. To eliminate false positives, data was then filtered by selecting only genes with a comparison number of ≥7. In addition, only genes passing the Mann-Whitney test ($P$ < 0.05) were selected. Finally, several genes were selected for additional validation by quantitative real-time PCR. The Affymetrix Analysis Center website was used for annotation of genes.

## Results

**CDDO-Im protects against aflatoxin-induced tumorigenesis in rat liver.** The chemopreventive potency of CDDO-Im was evaluated at doses ranging from 1 to 100 μmol/kg by measuring inhibition of formation of putative preneoplastic lesions (GST-P positive foci) in the liver of rats exposed to AFB$_1$. During the period of carcinogen dosing (weeks 2 and 3), toxicity of AFB$_1$ was observed as a failure of animals to gain weight (Fig. 3). Weekly weight gain was reduced by 36% ($P$ < 0.05) in rats treated with AFB$_1$ compared with vehicle controls. Treatment with CDDO-Im at doses of 3 to

30 μmol/kg provided protection against growth inhibition such that there was no longer a statistically significant difference in weight gain compared with rats not exposed to AFB$_1$. However, during week 1 of the dosing protocol (before receiving AFB$_1$), weight gain was inhibited by 25% at the 100 μmol/kg dose, indicating some toxicity at this high dose of CDDO-Im. At the termination of the experiment, mean body weights of each group were similar to the no AFB$_1$ group.

The number of GST-P positive foci was strikingly reduced at all doses of CDDO-Im. Data obtained from microscopic observation of GST-P positive lesions in the liver and calculated morphometric data are presented in Table 1. The number of GST-P positive foci per square centimeter of liver was reduced in a dose-dependent manner. At 1 μmol/kg, the number of foci per square centimeter of liver was reduced by 39% and at the highest dose no foci were observed. Additionally, all doses of CDDO-Im resulted in reduction of observed mean focal area. Because the statistical analysis of the two-dimensional data is inappropriate, the observed focal data were subjected to morphometric transformation, resulting in foci per unit volume of liver, mean focal diameter, and the volume percent of liver occupied by GST-P positive foci, a variable that is analogous to tumor burden. The foci per cubic-centimeter volume of liver were reduced at doses ranging from 3 to 100 μmol/kg, but there were no differences in mean focal diameter among these groups. Volume percent of liver occupied by GST-P positive foci is the most robust variable and is presented in Fig. 4. The lowest dose of CDDO-Im, 1 μmol/kg, reduced the hepatic focal burden (volume percent) of preneoplastic lesions by >85% and the highest dose, 100 μmol/kg, produced a >99% reduction. Each of the CDDO-Im dose groups was significantly different from the AFB$_1$-only group. Figure 4 also shows dose-response curves for two members of the dithiolethione class of cancer chemopreventive agents, 3*H*-1,2-dithiole-3-thione (D3T) and oltipraz, from a recent study described by Roebuck et al. (2) using an identical treatment protocol. These curves highlight the remarkably greater chemopreventive potency of CDDO-Im.

**CDDO-Im reduces levels of aflatoxin-DNA adducts in rat liver.** Pretreatment with CDDO-Im inhibits hepatic aflatoxin-DNA adduct formation at all doses studied (Fig. 5). Aflatoxin-DNA
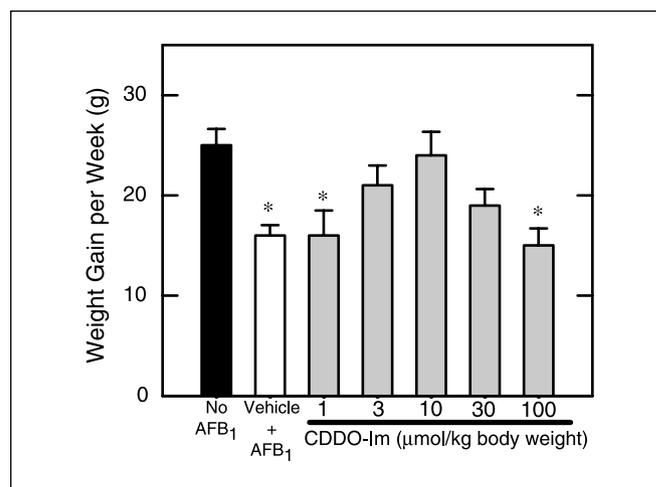


**Figure 3.** Protection by CDDO-Im against growth inhibition resulting from treatment with AFB$_1$ measured during weeks 2 and 3 of the hepatic foci inhibition protocol. *, $P$ < 0.05, compared with no AFB$_1$ group. Growth inhibition at 100 μmol/kg began before dosing with AFB$_1$, indicating that growth inhibition is due to toxicity associated with CDDO-Im.

**Table 1.** Chemoprevention of AFB$_1$-induced hepatocarcinogenesis by the triterpenoid CDDO-Im

| Observed data[*],[†] | | | Calculated morphometric data | |
|---|---|---|---|---|
| Group | GST-P (foci/cm$^2$) | Mean focal area (mm$^2$ × 100) | Foci/cm$^3$ liver | Focal diameter (μm) |
| No AFB$_1$ | 0.08 ± 0.08 | 1.04 | 5 ± 5 | 162 |
| AFB$_1$ | 10.96 ± 2.26 | 5.99 ± 1.25 | 668 ± 142 | 162 ± 21 |
| CDDO-Im (μmol/kg) | | | | |
| 1 | 6.70 ± 1.31 | 1.43 ± 0.27 | 746 ± 147 | 94 ± 10 |
| 3 | 2.30 ± 0.55 | 1.11 ± 0.48 | 318 ± 44[‡] | 75 ± 16 |
| 10 | 0.84 ± 0.07 | 0.97 ± 0.41 | 86 ± 23[‡],[§] | 133 ± 39 |
| 30 | 0.22 | 1.46 | 11[‡],[§] | 196 |
| 100 | 0 | — | 0[‡],[§] | — |

[*]Mean ± SE, $n = 5$.
[†]An average of 2 cm$^2$ liver tissue was examined per rat.
[‡]Statistically different ($P < 0.05$) than the 1 μmol/kg group.
[§]Statistically different ($P < 0.05$) than the AFB$_1$ group.

adduct levels were measured 2 hours after carcinogen dosing, the time of maximum DNA adduct burden. Levels of aflatoxin-$N^7$-guanine are reduced by ~40% to 90% over the range of 1 to 100 μmol/kg. Although all doses resulted in statistically significant reduction in DNA adduct levels, as in other studies (31), measurement of inhibition of aflatoxin-DNA adduct formation underestimates *in vivo* chemopreventive potency.

**CDDO-Im induces genes involved in aflatoxin detoxification.** Induction of phase 2 genes contributes to protection against aflatoxin hepatocarcinogenesis. GSTs conjugate aflatoxin-8,9-oxide to glutathione, thereby diverting the epoxide from interacting with DNA. AFAR reduces aflatoxin dialdehyde, a potentially cytotoxic metabolite, to aflatoxin monoalcohols and dialcohols. Shown in Table 2, a single low dose of CDDO-Im (1 μmol/kg) significantly increased levels of RNA transcripts in rat liver for *GSTA2*, *GSTA5*, *AFAR*, *EPHX1*, and *NQO1* at 6 hours after treatment. Cytochrome P450s activate AFB$_1$ to form the ultimate carcinogen aflatoxin-8,9-epoxide (32). *CYP2C11*, which is largely responsible for the activation of AFB$_1$ in rats (33), was not induced by CDDO-Im. A higher dose, 10 μmol/kg, is required for induction of *HMOX1*, a gene associated with triterpenoid action in other models (12). The highest dose, 30 μmol/kg, induced the genes mentioned above and also reduced transcript levels of *CYP2C11*. Two time points were examined with this dose of CDDO-Im. Treatment with 30 μmol/kg altered transcript levels at 6 and 24 hours for each gene except *HMOX1*. As shown previously in mice (12), *HMOX1* is highly induced at 6 hours, but returns to basal levels by 24 hours.

Induction of protein products was measured by immunoblot. AFAR and GSTA5 proteins were induced in rat liver 24 hours following treatment with CDDO-Im at a dose of 30 μmol/kg (Fig. 6). GSTA5 protein expression was induced 2.6-fold, a level comparable with RNA transcript induction. AFAR protein expression was induced to a lesser extent (8-fold) compared with RNA transcript levels (45-fold) at the same dose and time point.

**CDDO-Im induces phase 2 and antioxidant genes in an Nrf2-dependent manner.** The protective mechanisms induced by CDDO-Im were further investigated using microarray analysis.

Livers from wild-type and *Nrf2* knockout mice treated with 150 μmol CDDO-Im/kg were used for global gene expression analysis. This high dose of CDDO-Im was chosen to maximize response and facilitate characterization of subtle gene changes. This analysis highlighted over 1,000 induced or repressed genes. A complete description of these results will appear elsewhere, but a brief list of important phase 2 and antioxidant genes is provided in Table 3. CDDO-Im induced many genes in wild-type mice that were not induced in *Nrf2*-disrupted mice. Such genes are Nrf2-dependent and include *Nqo1*, *Txnrd1*, and *Gstm3*. Some genes, such as *Gsto1* and *Mgst3*, were induced in the wild-type and *Nrf2* knockout mice, indicating that these responses are Nrf2 independent. Other genes, such as *Gsta2* and *Gsta4*, are partially dependent on Nrf2 and result in differential inductive responses in wild-type and *Nrf2* knockout mice.
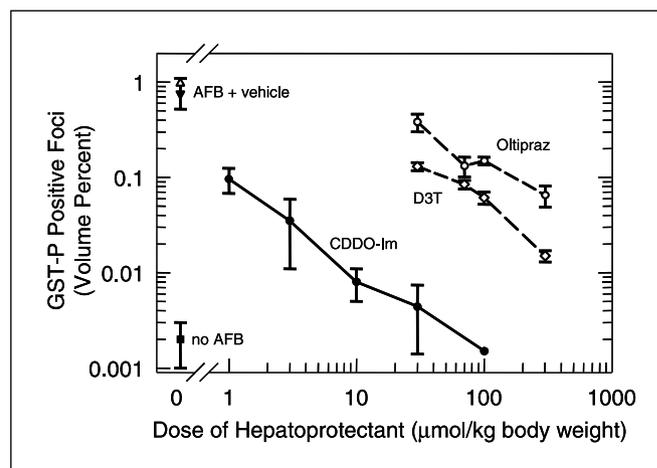


**Figure 4.** Protection by CDDO-Im against AFB$_1$-induced GST-P positive foci formation. Foci were not detected in some animals given the highest doses of CDDO-Im. Values of $L / 2$ were inserted for all zero values. D3T and oltipraz dose-response curves are provided for comparison (2). ▼, AFB$_1$ + vehicle group concurrent with CDDO-Im groups; ▲, AFB$_1$ + vehicle group concurrent with D3T and oltipraz groups. *Points,* mean ($n = 5$); *bars,* SE.
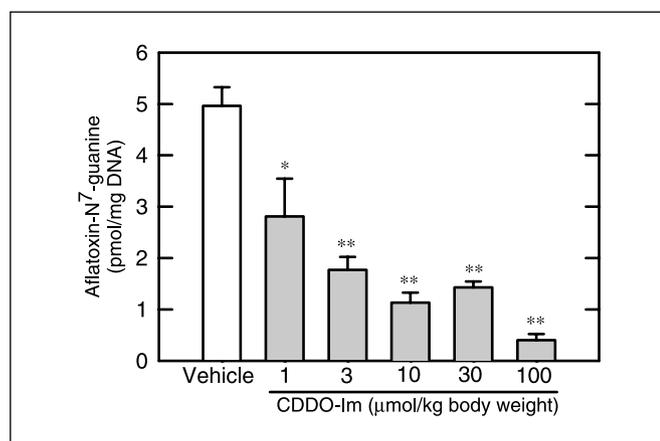
**Figure 5.** Protection by CDDO-Im against aflatoxin-DNA adduct formation. **, $P < 0.001$, compared with vehicle. *, $P < 0.02$, compared with vehicle. *Columns,* mean ($n = 4$); *bars,* SE.

## Discussion

The rat model of aflatoxin-induced hepatic tumorigenesis used in this study is a valuable tool for the evaluation of new classes of chemopreventive agents and the development of structure-activity comparisons. This model is particularly powerful in that it allows for a highly quantitative evaluation of the number and size, and hence a volumetric estimate of tumor burden, in a short-term assay of preneoplastic lesions using modest numbers of animals. Such quantitative models allow for full dose-response determination of the chemopreventive efficacy and potency of candidate agents. Moreover, decades of mechanistic studies on aflatoxin hepatocarcinogenesis in rodents provide a clear perspective on the roles of carcinogen metabolism, DNA damage, and hepatotoxicity on etiopathogenesis, thereby defining suitable molecular targets for interventions and intermediate markers for adjudging efficacy. Our utilization of the model has shown concordant protective effects of chemopreventive agents on hepatic DNA adduct burden, preneoplastic lesion formation (GST-P positive

foci), and hepatocarcinogenesis (24, 34). Lastly, the model can inform the development of chemopreventive agents for use in human populations because of the etiologic relevance of aflatoxins to human cancer. The utility of this model has been shown in the preclinical development of the dithiolethione class of chemopreventive agents. Extensive dose-response studies were conducted in this bioassay to further characterize structure-activity relationships for dithiolethione analogues of oltipraz. These studies identified the dithiolethione nucleus of the molecule as the crucial portion responsible for chemoprotective activity, highlighting D3T as the most potent and effective member of the class (35). Heretofore, dithiolethiones represented the most potent inhibitors of aflatoxin-induced tumorigenesis studied. Treatment with oltipraz or D3T at a dose of 30 μmol/kg provides 60% and 85% inhibition of hepatic focal burden, respectively (2). Treatment with other chemical classes of agents, such as the antioxidants ethoxyquin, butylated hydroxyanisole, or butylated hydroxytoluene, although effective anticarcinogens, resulted in far less potent inhibition of tumorigenesis. These agents were administered in the diet and resulted in reduced tumor incidences at doses of 0.5% ethoxyquin (36), 0.1% butylated hydroxyanisole, or 0.1% butylated hydroxytoluene (37).

Evaluation of CDDO-Im in this rat model allows us to compare the potency of this triterpenoid to that of D3T, the most potent member of the dithiolethione class and oltipraz, an agent with demonstrable effect on aflatoxin disposition in humans. In this study, we show that CDDO-Im provides an 85% reduction of hepatic focal burden following treatment with a dose of 1 μmol/kg. This outcome represents a 30-fold improvement in chemopreventive potency compared with D3T and a 100-fold enhancement of potency compared with oltipraz. In as much as *in vitro* studies indicate a broad concentration range of activities among triterpenoid analogues, future studies in this aflatoxin tumorigenesis model will be well suited to probe structure-activity relationships *in vivo* as well as the underlying mechanisms that result in protection.

The protection provided by CDDO-Im is likely achieved through interaction with signaling pathways mediated by the transcription factor Nrf2. Expression of genes contributing to aflatoxin detoxication, namely, *AFAR* and *GSTs*, are elevated at all doses of CDDO-Im tested. Western blot analyses indicated that protein levels were also elevated for the gene products. The extreme potency of CDDO-Im makes it unlikely that protection is caused by inhibition of cytochrome P450–mediated bioactivation

**Table 2.** Dose-dependent changes in mRNA levels measured by quantitative reverse transcription-PCR in rat liver after treatment with CDDO-Im

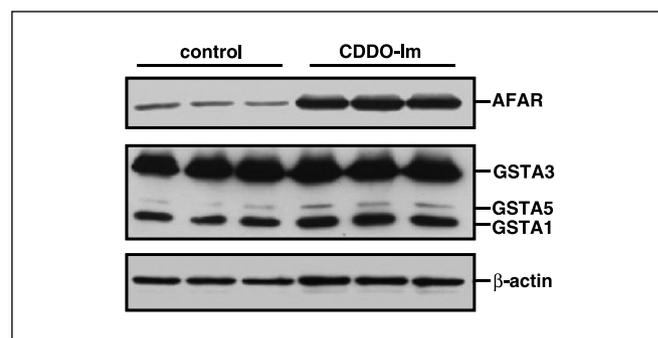| Gene | Fold induction | | | | |
| --- | --- | --- | --- | --- | --- |
| | 1 μmol/kg (6 h) | 3 μmol/kg (6 h) | 10 μmol/kg (6 h) | 30 μmol/kg (6 h) | 30 μmol/kg (24 h) |
| NQO1 | 5.0* | 6.6* | 8.4* | 10.5* | 12.2* |
| GSTA2 | 3.1* | 3.6* | 4.5* | 3.1* | 3.8* |
| GSTA5 | 2.0* | 2.0* | 2.6* | 2.3* | 3.4* |
| AFAR | 13.3* | 21.7* | 37.7* | 55.5* | 44.7* |
| EPHX1 | 3.6* | 3.9* | 5.4* | 4.4* | 4.0* |
| HMOX1 | 1.1 | 1.3 | 2.0* | 5.9* | 0.9 |
| CYP2C11 | 0.7 | 1.2 | 0.8 | 0.7* | 0.3* |

*$P < 0.05$ compared with vehicle control.



**Figure 6.** Induction of hepatic AFAR and GSTA5 proteins after treatment with CDDO-Im. Each lane contains 30 μg of cytosolic protein prepared from livers of three rats treated with either vehicle or 30 μmol/kg of CDDO-Im.

**2492**

**Table 3.** Microarray analysis of the effect of Nrf2 genotype on expression of phase 2 and antioxidant genes by CDDO-Im in mouse liver

| Phase 2 and antioxidant genes | Description | Fold-induction | |
|---|---|---|---|
| | | Wild type | Nrf2−/− |
| Ephx1 | Epoxide hydrolase 1, microsomal | 4.9 | 2.3 |
| Ftl1 | Ferritin light chain 1 | 2.0 | * |
| Ftl2 | Ferritin light chain 2 | 2.3 | * |
| Gclc | Glutamate-cysteine ligase, catalytic subunit | 7.1 | 2.6 |
| Gclm | Glutamate-cysteine ligase, modifier subunit | 1.9 | * |
| Gsr | Glutathione reductase 1 | 3.7 | * |
| Gsta2 | Glutathione S-transferase, alpha 2 | 91.2 | 8.9 |
| Gsta3 | Glutathione S-transferase, alpha 3 | 6.4 | 11.3 |
| Gsta4 | Glutathione S-transferase, alpha 4 | 11.5 | 2.8 |
| Gstm1 | Glutathione S-transferase, mu 1 | 6.9 | 2.6 |
| Gstm2 | Glutathione S-transferase, mu 2 | 3.6 | 1.7 |
| Gstm3 | Glutathione S-transferase, mu 3 | 10.6 | * |
| Gstm4 | Glutathione S-transferase, mu 4 | 8.4 | * |
| Gstm6 | Glutathione S-transferase, mu 6 | 4.4 | * |
| Gsto1 | Glutathione S-transferase, omega 1 | 2.8 | 3.8 |
| Gstp1 | Glutathione S-transferase, pi 1 | 1.7 | * |
| Gstt1 | Glutathione S-transferase, theta 1 | † | 1.6 |
| Gstt2 | Glutathione S-transferase, theta 2 | † | 2.1 |
| Mgst3 | Microsomal glutathione S-transferase 3 | 2.5 | 2.1 |
| Nqo1 | NAD(P)H dehydrogenase, quinone 1 | 6.1 | * |
| Txn1 | Thioredoxin 1 | 1.8 | * |
| Txnrd1 | Thioredoxin reductase 1 | 2.5 | * |

*Not different from vehicle control in Nrf2-disrupted (Nrf2−/−) mice.
†Not different from vehicle control in wild-type mice.

of aflatoxin as seen with oltipraz (38). However, further studies will be necessary to fully characterize any potential alterations in cytochrome P450-mediated metabolism. Treatment with CDDO-Im results in substantial inhibition of DNA adduct formation following exposure to aflatoxin, although as seen previously with dithiolethiones (31) the extent of reduction of adduct burden by CDDO-Im underestimates inhibition of tumorigenesis. Such outcomes suggest that additional components of the hepatocarcinogenic process, such as hepatotoxicity, may also be affected by the triterpenoid. The involvement of Nrf2 in the protective actions of CDDO-Im can be inferred from our studies. Antioxidant response elements, which bind Nrf2, are found in the promoters of rat *AFAR* (39) and GST isoforms (40). In addition, microarray analysis comparing hepatic expression patterns in wild-type and *Nrf2*-disrupted mice following treatment with CDDO-Im show that protective genes, such as *Gstp1, Nqo1,* and *Txnrd1* are not induced in knockout mice. It is important to note, however, that not all CDDO-Im–inducible genes are regulated through the Nrf2 pathway. Genes such as *Ephx1* and *Mgst3* are induced in both genotypes of mice. The contributions of these Nrf2-independent pathways to protection in this model are unclear at present. Nonetheless, the unparalleled potency of CDDO-Im *in vivo* highlights the chemopreventive promise of targeting Nrf2 pathways with triterpenoids.

The striking protection achieved in this model indicates that triterpenoids warrant further examination as chemopreventive agents against hepatocarcinogenesis in humans. However, the potent effects on phase 2 enzyme induction combined with the anti-inflammatory properties of these compounds make them high-priority agents for prevention in other settings as well. Triterpenoids could be effective chemopreventive agents against cancers with a strong link to inflammation, such as colon, prostate, and gastric cancers. Because Nrf2 is implicated in the regulation of many categories of genes involved in protection, the activation of Nrf2 signaling caused by treatment with CDDO-Im could provide protection against multiple mechanisms that lead to carcinogenesis. Further pharmacokinetic and pharmacodynamic studies with CDDO-Im are needed to characterize the localization and extent of induced protective pathways. Such investigations could suggest additional sites of chemopreventive action. Previous studies (12) suggest that the cytoprotective mechanisms induced by treatment with CDDO and CDDO-Im could also have implications for diseases such as Alzheimer's, diabetes, asthma, acute renal failure, and atherosclerosis.

## Acknowledgments

# References

1. Kensler TW, Helzlsouer KJ. Oltipraz: clinical opportunities for cancer chemoprevention. J Cell Biochem Suppl 1995;22:101–7.
2. Roebuck BD, Curphey TJ, Li Y, et al. Evaluation of the cancer chemopreventive potency of dithiolethione analogs of oltipraz. Carcinogenesis 2003;24:1919–28.
3. Kwak MK, Egner PA, Dolan PM, et al. Role of phase 2 enzyme induction in chemoprotection by dithiolethiones. Mutat Res 2001;480–1:305–15.
4. Gupta E, Olopade OI, Ratain MJ, et al. Pharmacokinetics and pharmacodynamics of oltipraz as a chemopreventive agent. Clin Cancer Res 1995;1:1133–8.
5. O'Dwyer PJ, Szarka CE, Yao KS, et al. Modulation of gene expression in subjects at risk for colorectal cancer by the chemopreventive dithiolethione oltipraz. J Clin Invest 1996;98:1210–7.
6. Wang JS, Shen X, He X, et al. Protective alterations in phase 1 and 2 metabolism of aflatoxin B1 by oltipraz in residents of Qidong, People's Republic of China. J Natl Cancer Inst 1999;91:347–54.
7. Motohashi H, Yamamoto M. Nrf2-Keap1 defines a physiologically important stress response mechanism. Trends Mol Med 2004;10:549–57.
8. Kwak MK, Wakabayashi N, Itoh K, Motohashi H, Yamamoto M, Kensler TW. Modulation of gene expression by cancer chemopreventive dithiolethiones through the Keap1-Nrf2 pathway. Identification of novel gene clusters for cell survival. J Biol Chem 2003;278:8135–45.
9. Ramos-Gomez M, Kwak MK, Dolan PM, et al. Sensitivity to carcinogenesis is increased and chemoprotective efficacy of enzyme inducers is lost in nrf2 transcription factor-deficient mice. Proc Natl Acad Sci U S A 2001;98:3410–5.
10. Dinkova-Kostova AT, Liby KT, Stephenson KK, et al. Extremely potent triterpenoid inducers of the phase 2 response: correlations of protection against oxidant and inflammatory stress. Proc Natl Acad Sci U S A 2005;102:4584–9.
11. Haridas V, Hanausek M, Nishimura G, et al. Triterpenoid electrophiles (avicins) activate the innate stress response by redox regulation of a gene battery. J Clin Invest 2004;113:65–73.
12. Liby K, Hock T, Yore MM, et al. The synthetic triterpenoids, CDDO and CDDO-imidazolide, are potent inducers of heme oxygenase-1 and Nrf2/ARE signaling. Cancer Res 2005;65:4789–98.
13. Lapillonne H, Konopleva M, Tsao T, et al. Activation of peroxisome proliferator-activated receptor γ by a novel synthetic triterpenoid 2-cyano-3,12-dioxooleana-1,9-dien-28-oic acid induces growth arrest and apoptosis in breast cancer cells. Cancer Res 2003;63:5926–39.
14. Konopleva M, Tsao T, Estrov Z, et al. The synthetic triterpenoid 2-cyano-3,12-dioxooleana-1,9-dien-28-oic acid induces caspase-dependent and -independent apoptosis in acute myelogenous leukemia. Cancer Res 2004;64:7927–35.
15. Suh N, Wang Y, Honda T, et al. A novel synthetic oleanane triterpenoid, 2-cyano-3,12-dioxoolean-1,9-dien-28-oic acid, with potent differentiating, antiproliferative, and anti-inflammatory activity. Cancer Res 1999;59:336–41.
16. Place AE, Suh N, Williams CR, et al. The novel synthetic triterpenoid, CDDO-imidazolide, inhibits inflammatory response and tumor growth *in vivo*. Clin Cancer Res 2003;9:2798–806.
17. Kwak MK, Itoh K, Yamamoto M, Sutter TR, Kensler TW. Role of transcription factor Nrf2 in the induction of hepatic phase 2 and antioxidative enzymes *in vivo* by the cancer chemoprotective agent, 3*H*-1,2-dithiole-3-thione. Mol Med 2001;7:135–45.
18. Honda T, Honda Y, Favaloro FG, Jr., et al. A novel dicyanotriterpenoid, 2-cyano-3,12-dioxooleana-1,9(11)-dien-28-onitrile, active at picomolar concentrations for inhibition of nitric oxide production. Bioorg Med Chem Lett 2002;12:1027–30.
19. Honda T, Rounds BV, Bore L, et al. Synthetic oleanane and ursane triterpenoids with modified rings A and C: a series of highly active inhibitors of nitric oxide production in mouse macrophages. J Med Chem 2000;43:4233–46.
20. Honda T, Rounds BV, Gribble GW, Suh N, Wang Y, Sporn MB. Design and synthesis of 2-cyano-3,12-dioxoolean-1,9-dien-28-oic acid, a novel and highly active inhibitor of nitric oxide production in mouse macrophages. Bioorg Med Chem Lett 1998;8:2711–4.
21. Kensler TW, Egner PA, Trush MA, Bueding E, Groopman JD. Modification of aflatoxin B1 binding to DNA *in vivo* in rats fed phenolic antioxidants, ethoxyquin and a dithiothione. Carcinogenesis 1985;6:759–63.
22. Egner PA, Yu X, Johnson JK, et al. Identification of aflatoxin M1-N7-guanine in liver and urine of tree shrews and rats following administration of aflatoxin B1. Chem Res Toxicol 2003;16:1174–80.
23. Pugh TD, King JH, Koen H, et al. Reliable stereological method for estimating the number of microscopic hepatocellular foci from their transections. Cancer Res 1983;43:1261–8.
24. Kensler TW, Groopman JD, Eaton DL, Curphey TJ, Roebuck BD. Potent inhibition of aflatoxin-induced hepatic tumorigenesis by the monofunctional enzyme inducer 1,2-dithiole-3-thione. Carcinogenesis 1992;13:95–100.
25. Maxuitenko YY, Curphey TJ, Kensler TW, Roebuck BD. Protection against aflatoxin B1-induced hepatic toxicity as short-term screen of cancer chemopreventive dithiolethiones. Fundam Appl Toxicol 1996;32:250–9.
26. Hornung RW, Reed LD. Estimation of average concentration in the presence of nondetectable values. Appl Occup Environ Hyg 1990;5:46–51.
27. Livak KJ, Schmittgen TD. Analysis of relative gene expression data using real-time quantitative PCR and the $2(-\Delta\Delta C(T))$ method. Methods 2001;25:402–8.
28. Hayes JD, Mantle TJ. Use of immuno-blot techniques to discriminate between the glutathione *S*-transferase Yf, Yk, Ya, Yn/Yb and Yc subunits and to study their distribution in extrahepatic tissues. Evidence for three immunochemically distinct groups of transferase in the rat. Biochem J 1986;233:779–88.
29. Knight LP, Primiano T, Groopman JD, Kensler TW, Sutter TR. cDNA cloning, expression and activity of a second human aflatoxin B1-metabolizing member of the aldo-keto reductase superfamily, AKR7A3. Carcinogenesis 1999;20:1215–23.
30. Hayes JD, Nguyen T, Judah DJ, Petersson DG, Neal GE. Cloning of cDNAs from fetal rat liver encoding glutathione *S*-transferase Yc polypeptides. The Yc2 subunit is expressed in adult rat liver resistant to the hepatocarcinogen aflatoxin B1. J Biol Chem 1994;269:20707–17.
31. Kensler TW, Groopman JD, Sutter TR, Curphey TJ, Roebuck BD. Development of cancer chemopreventive agents: oltipraz as a paradigm. Chem Res Toxicol 1999;12:113–26.
32. Eaton DL, Gallagher EP. Mechanisms of aflatoxin carcinogenesis. Annu Rev Pharmacol Toxicol 1994;34:135–72.
33. Ishii K, Maeda K, Kamataki T, Kato R. Mutagenic activation of aflatoxin B1 by several forms of purified cytochrome P-450. Mutat Res 1986;174:85–8.
34. Roebuck BD, Liu YL, Rogers AE, Groopman JD, Kensler TW. Protection against aflatoxin B1-induced hepatocarcinogenesis in F344 rats by 5-(2-pyrazinyl)-4-methyl-1,2-dithiole-3-thione (oltipraz): predictive role for short-term molecular dosimetry. Cancer Res 1991;51:5501–6.
35. Kensler TW, Egner PA, Dolan PM, Groopman JD, Roebuck BD. Mechanism of protection against aflatoxin tumorigenicity in rats fed 5-(2-pyrazinyl)-4-methyl-1,2-dithiol-3-thione (oltipraz) and related 1,2-dithiol-3-thiones and 1,2-dithiol-3-ones. Cancer Res 1987;47:4271–7.
36. Cabral JR, Neal GE. The inhibitory effects of ethoxyquin on the carcinogenic action of aflatoxin B1 in rats. Cancer Lett 1983;19:125–32.
37. Williams GM, Tanaka T, Maeura Y. Dose-related inhibition of aflatoxin B1 induced hepatocarcinogenesis by the phenolic antioxidants, butylated hydroxyanisole and butylated hydroxytoluene. Carcinogenesis 1986;7:1043–50.
38. Buetler TM, Bammler TK, Hayes JD, Eaton DL. Oltipraz-mediated changes in aflatoxin B1 biotransformation in rat liver: implications for human chemointervention. Cancer Res 1996;56:2306–13.
39. Ellis EM, Slattery CM, Hayes JD. Characterization of the rat aflatoxin B1 aldehyde reductase gene, AKR7A1. Structure and chromosomal localization of AKR7A1 as well as identification of antioxidant response elements in the gene promoter. Carcinogenesis 2003;24:727–37.
40. Nguyen T, Rushmore TH, Pickett CB. Transcriptional regulation of a rat liver glutathione *S*-transferase Ya subunit gene. Analysis of the antioxidant response element and its activation by the phorbol ester 12-*O*-tetradecanoylphorbol-13-acetate. J Biol Chem 1994;269:13656–62.